EMBO reports

scientific report

Overgrowth of a mouse model of Simpson–Golabi–Behmel syndrome is partly mediated by Indian Hedgehog

Mariana I. Capurro, Fuchuan Li & Jorge Filmus[+]

Division of Molecular and Cell Biology, Sunnybrook Research Institute and Department of Medical Biophysics, University of Toronto, Toronto, Ontario, Canada

Loss-of-function mutations of Glypican 3 (*Gpc3*) cause the Simpson–Golabi–Behmel overgrowth syndrome (SGBS), and developmental overgrowth is observed in *Gpc3*-null mice, a mouse model for SGBS. We recently reported that GPC3 inhibits Hedgehog (Hh) signalling by inducing its endocytosis and degradation. Here, we show that the developmental overgrowth observed in *Gpc3*-null mice is, at least in part, a consequence of the hyperactivation of the Hh pathway. We bred *Gpc3*-null mice with mice that are Hh signalling-deficient owing to the lack of Indian Hh (Ihh), one of the three mammalian Hhs. We found that the *Gpc3*-null mice showed a 29.9% overgrowth in an Ihh wild-type background, whereas an Ihh-null background partly rescues the overgrowth caused by the lack of *Gpc3* as the double mutants were 19.8% bigger than the Ihh-null mice. Consistent with the role of GPC3 in Hh endocytosis and degradation, the *Gpc3*-null mice show increased levels of Ihh protein and signalling, but similar levels of Ihh messenger RNA.

Keywords: Glypicans; Hedgehog; Simpson–Golabi–Behmel syndrome; overgrowth; heparan sulphate proteoglycans

EMBO reports (2009) **10**, 901–907. doi:10.1038/embor.2009.98

INTRODUCTION

Several genetic studies have shown that Glypican 3 (*Gpc3*), one of six mammalian glypicans, has a crucial role in the regulation of body size. First, loss-of-function mutations of *Gpc3* cause the Simpson–Golabi–Behmel overgrowth syndrome (SGBS; Pilia *et al*, 1996); second, *Gpc3*-deficient mice show developmental overgrowth (Cano-Gauci *et al*, 1999; Paine-Saunders *et al*, 2000; Chiao *et al*, 2002); and third, *Gpc3* polymorphisms have a significant impact on the body size of mice (Oliver *et al*, 2005).

Division of Molecular and Cell Biology, Sunnybrook Research Institute and Department of Medical Biophysics, University of Toronto, 2075 Bayview Avenue Toronto, Ontario, M4N3M5 Canada

[+]Corresponding author. Tel: +1 416 480 6100 ext. 3350; Fax: +1 416 480 5703; E-mail: jorge.filmus@sri.utoronto.ca

Received 1 October 2008; revised 8 April 2009; accepted 9 April 2009; published online 10 July 2009

As insulin-like growth factors (IGFs) have a determinant role in the regulation of body size, it was initially proposed that GPC3 inhibits embryonic growth by acting as a negative regulator of these growth factors (Pilia *et al*, 1996). However, several genetic and biochemical studies have shown that GPC3 does not interact with the IGF signalling pathway (Cano-Gauci *et al*, 1999; Chiao *et al*, 2002; Song *et al*, 2005).

Our laboratory recently tested the hypothesis that GPC3 could regulate embryonic growth by acting as a negative regulator of Hedgehog (Hh) signalling. Glypicans have already been implicated in the regulation of Hh activity by genetic studies in *Drosophila* (Desbordes & Sanson, 2003; Lum *et al*, 2003; Han *et al*, 2004). In addition, there is strong evidence that the Hh signalling pathway has a crucial role in the regulation of body size: germ-line mutations in humans and mice that activate the Hh signalling pathway induce significant overgrowth (Gorlin, 1995; Milenkovic *et al*, 1999).

As a result of the studies that we performed to test the hypothesis that GPC3 acts as a negative regulator of Hh signalling, we have recently shown that the expression of Hh target genes is significantly increased in *Gpc3*-null mice (Capurro *et al*, 2008). We also showed that GPC3 competes with Patched (PTC), the Hh receptor, for Hh binding. The binding of Hh to GPC3 triggers the endocytosis and degradation of the complex, reducing the levels of Hh available for binding to PTC (Capurro *et al*, 2008). These results strongly support our hypothesis; however, definitive proof that the Hh signalling pathway mediates the role of GPC3 as a regulator of body size requires the demonstration that the overgrowth observed in *Gpc3*-null mice can be completely eliminated in mice in which the Hh signalling pathway has been abrogated, or that it can be partly reduced in mice with suboptimal Hh signalling. Unfortunately, mice lacking Hh signalling, such as the Smoothened-null mice, die at a very early stage of development (embryonic day (E)9.5; Zhang *et al*, 2001), well before GPC3 starts to have a regulatory role with regard to body size (Chiao *et al*, 2002). The only alternative, therefore, was to breed *Gpc3*-null mice with mice that show suboptimal Hh activity.

Table 1 | Breeding information

Phenotype	*Genotype Gpc3/Ihh*	*Number of mice*	*Expected frequency (%)**	*Observed frequency (%)*	*Relative body weight‡*
Normal	++/++ ++/+− +Y/++ +Y/+−	48	37.5	38.09	1 ± 0.0075
Ihh KO	++/−− +Y/−−	6	12.5	4.76	0.754 ± 0.0161
Gpc3 KO	−Y/++ −Y/+−	39	18.75	30.95	1.299 ± 0.0157
Double KO	−Y/−−	4	6.25	3.17	0.903 ± 0.0419

Gpc3, glypican 3; *Ihh*, Indian hedgehog; KO, knock-out. Breeding data (Female $Gpc3^{+/-}$; $Ihh^{+/-}$ × Male $Gpc3^{+/Y}$; $Ihh^{+/-}$). Statistical analysis was performed by Student's *t*-test (unpaired) and the differences between all groups were highly significant: $P = 0.0013$ for normal-double KO and $P = 0.0048$ for *Ihh* KO-double KO pairs; $P < 0.0001$ for all other pairs. *The expected frequency does not add up to 100% as the 25% correspondent to *Gpc3* heterozygous females ($Ihh^{+/+}$, $^{+/-}$ or $^{-/-}$) were not included in the study. The intermediate body weight reported for *Gpc3* heterozygous females produces smaller differences in body size and data more difficult to analyse. ‡Relative body weights (average ± s.d.) were calculated considering as 1 the average wild-type embryo weight per litter.

Three Hhs have been identified in mammals: Sonic (Shh), widely expressed in the embryo; Indian (Ihh), mainly expressed by developing bones; and Desert (Dhh), expressed only in the testis (Nieuwenhuis & Hui, 2005). *Shh* and *Ihh* double mutants die at E8.5 (Zhang *et al*, 2001), probably due to the complete lack of Hh signalling in most tissues. However, a proportion of *Ihh* single mutants are viable at birth, although they show a phenotype that clearly indicates suboptimal Hh activity (St-Jacques *et al*, 1999).

Here, we investigated the genetic interaction between GPC3 and the Hh signalling pathway by generating double-mutant mice lacking *Gpc3* and *Ihh*. Ihh acts locally to stimulate the development of the endochondral skeleton. It is produced by pre-hypertrophic and early hypertrophic chondrocytes, and signals in both chondrocytes and the overlying perichondrium (St-Jacques *et al*, 1999; Kronenberg, 2003; Ehlen *et al*, 2006). *Ihh*-null mice show a severe growth deficiency in the endochondral skeleton as a result of a reduced chondrocyte proliferation and maturation, as well as osteoblast formation (St-Jacques *et al*, 1999). Half of the *Ihh*-null embryos die between E10.5 and E12.5 owing to circulatory problems; the other half undergo complete development but are 20% smaller than normal littermates by E17.5–E18.5 (St-Jacques *et al*, 1999). Here, we report that an *Ihh*-null background partly rescues the overgrowth phenotype caused by the lack of *Gpc3*, providing conclusive genetic evidence that the Hh signalling pathway mediates, at least in part, the regulatory activity of GPC3 on embryonic growth.

RESULTS AND DISCUSSION

To generate double mutants lacking *Gpc3* and *Ihh* (double knock-out (DKO)) in a C57/BL6 genetic background, we bred $Gpc3^{+/-}$; $Ihh^{+/-}$ females with $Gpc3^{+/Y}$ and $Ihh^{+/-}$ males. From 16 breeding pairs we collected a total of 126 E16.5–E18.5 embryos, and obtained four DKO embryos, at a frequency of 3.17% that is lower than the expected Mendelian ratio (6.25%; Table 1). However, taking into account that 50% of *Ihh*-null embryos were reported to die around 10.5–12.5 days *post coitum* (dpc), the recovery rate was at the expected ratio (3.125%). Although phenotypically normal embryos were obtained at the expected frequency, *Gpc3*-null mice were identified at a higher than expected ratio (Table 1). This might be the consequence of an increased viability owing to the overgrowth phenotype as *Gpc3* knock-out-associated lethality occurs after birth. The *Ihh*-null mice, conversely, were obtained at a lower than expected frequency (4.76% versus 6.25%, considering the reported lethality between 10.5 and 12.5 dpc). This is probably due to the increased lethality in a C57BL/6 background.

We compared the weights of E16.5–E18.5 *Gpc3*-null and normal littermate embryos in *Ihh* wild-type and knock-out backgrounds. It has already been established that during this stage of development the relative effect of the lack of *Gpc3* and of the inactivation of Hh signalling on embryo size is constant (Cano-Gauci *et al*, 1999; Milenkovic *et al*, 1999). Fig 1 shows that *Gpc3* knock-out mice showed a 29.9% overgrowth compared with *Gpc3* wild-type mice in an *Ihh* wild-type background, whereas the *Gpc3* knock-out mice were only 19.8% bigger in an *Ihh*-null background. This result clearly indicates that the Hh signalling pathway mediates, at least in part, the regulatory activity of GPC3 on embryonic size. The *Gpc3* knock-out mice still show some overgrowth in the *Ihh*-null background, but this is expected because the Hh signalling pathway is still active in the *Ihh*-null mice due to the presence of Shh. In fact, as we have shown in *Gpc3* knock-out mice, Shh levels were higher in the *Gpc3*/*Ihh* DKOs compared with the wild-type mice (Fig 1B). As a control, we have shown that the $Ihh^{-/-}$ mutation does not alter Shh levels as a compensatory mechanism (Fig 1B). However, at this point in time we cannot discard the possibility that, in addition to Hh, other growth factors such as bone morphogenetic proteins (BMPs) or Wnts could also mediate some of the regulatory activity of GPC3 on embryonic growth. However, we consider this possibility unlikely, as there is no genetic evidence suggesting that the signalling pathways triggered by Wnts or BMPs are involved in the regulation of embryo size.

We have shown previously that GPC3 can inhibit the activity of Shh and Ihh in a *Gli*-reporter luciferase assay (Capurro *et al*, 2008). In addition, we showed that GPC3 competes with PTC for Shh binding at the cell membrane, and that the binding of Shh to GPC3 triggers the endocytosis and degradation of the GPC3–Shh complex (Capurro *et al*, 2008). However, the mechanism by which GPC3 inhibits Ihh activity was not investigated. To characterize such a mechanism, we first studied the interaction

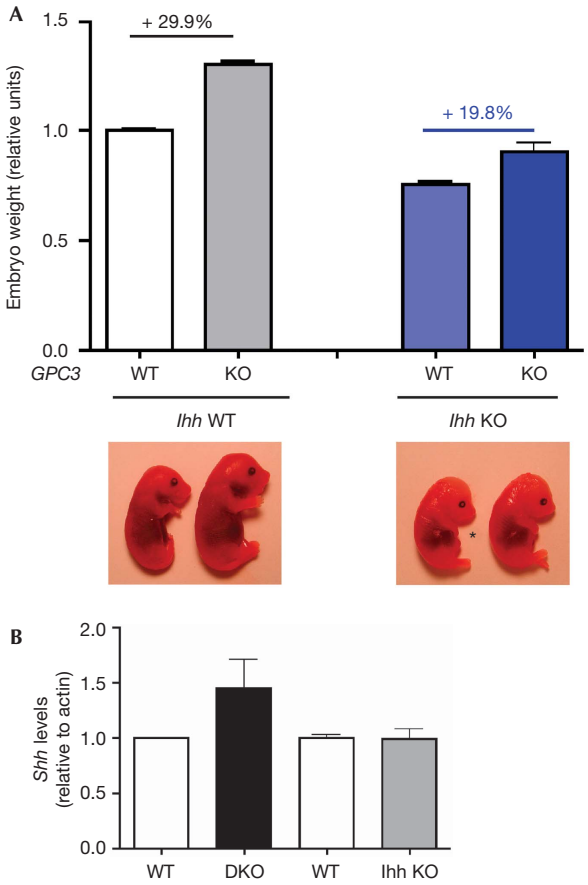

Fig 1 | Analysis of Glypican 3-null and normal littermate embryos in an Indian hedgehog wild-type and null background. (**A**) Top: Relative body weights of embryos of the indicated genotype. The average wild-type weight per litter was arbitrarily assigned the value of 1. Bars represent average relative weight + s.d. $n = 48$, 39, 6 and 4 for *GPC3* WT and KO in *Ihh* WT and null background, respectively. Bottom: Gross morphology of embryonic day 17.5 embryos. Note the diminished limbs in *Ihh* knock-out embryos (asterisk). (**B**) Increased Shh levels in *Gpc3-Ihh* double knock-out (DKO) mice. Western blot analysis of Shh levels in whole-embryo lysates of *Ihh* knock-out or DKO mice, compared with the correspondent normal littermates, was carried out using actin as loading control. Bands were scanned and quantified by densitometry. Average density + s.d. of Shh/actin ratio is shown. In all five independent litters were analysed. DKO, double knock-out; GPC3, Glypican 3; Ihh, Indian hedgehog; KO, knock-out; Shh, sonic hedgehog; WT, wild type.

between GPC3 and Ihh at the cell surface. To this end, a cell-binding assay using ^{125}I-Ihh was carried out. As shown in Fig 2A, GPC3-expressing cells bound significantly more ^{125}I-Ihh than vector control-expressing cells. In addition, the difference in ^{125}I-Ihh binding between GPC3-transfected and vector-transfected cells was even higher when specific binding was measured (Fig 2B). Next, the binding of Ihh to GPC3 was characterized by surface plasmon resonance (SRP) analysis. Fig 2C shows that Ihh binds with high affinity to GPC3, indicating the existence of a direct Ihh–GPC3 interaction. We also investigated whether the GPC3-induced inhibition of Hh signalling depends on the presence of CAM-related/downregulated by oncogenes (CDO) or Hedgehog-interacting protein (HIP), two proteins that regulate the interaction of Hh with PTC1. To this end, we investigated the effect of small interference RNAs (siRNAs) targeting CDO or hedgehog in luciferase reporter expression assays. As shown in Fig 2D, the siRNAs did not alter the degree of GPC3-induced inhibition of Hh signalling, indicating that this activity of GPC3 is independent of CDO and HIP.

If GPC3 were able to induce endocytosis and degradation of Ihh after binding, as has been shown for Shh, *Gpc3* knock-out embryos should show higher levels of Ihh. To test this, Ihh levels in whole-embryo lysates were assessed by Western blot analysis. We found that *Gpc3*-null mice show significantly more Ihh than wild-type littermates (Fig 2E). To confirm that the changes observed in the *Gpc3*-mutant mice only take place at the protein level, *Ihh* messenger RNA (mRNA) was quantified by real-time PCR after reverse transcriptase (RT–PCR). Consistent with our model, similar levels of *Ihh* mRNA were detected in *Gpc3*-null embryos and normal littermates (Fig 2F). Altogether, these experiments support a model in which GPC3 inhibits Ihh signalling by binding to this growth factor at the cell surface, inducing its endocytosis and degradation.

Ihh$^{-/-}$ mice show a severe growth deficiency, with skeletal elements that are around 20% of the normal size at birth (St-Jacques *et al*, 1999). In developing bones, Ihh is mainly synthesized by the prehypertrophic chondrocyte domain of the growth plate, where it acts to increase chondrocyte proliferation and provides crucial signals to the perichondrium (Kronenberg, 2003). Interestingly, GPC3 expression in developing bones overlaps with Ihh localization (Viviano *et al*, 2005). If GPC3 triggers Ihh degradation, we would expect the bones of *Gpc3* knock-out mice to show higher amounts of Ihh. Therefore, we decided to assess Ihh levels in tissue sections of bones from the limbs and spine of *Gpc3*-null and normal littermates by immunohistochemistry. We found that, compared with normal littermates, *Gpc3*-deficient mice show significantly higher Ihh levels in the cartilage primordium of the ribs and perichondrium (Fig 3A), as well as in the prehypertrophic chondrocyte domain of the growth plates of the femur (Fig 3B). The fact that similar levels of *Ihh* mRNA were detected in bones from *Gpc3*-null and normal littermates embryos (Fig 3C) provides additional evidence supporting our proposition that *Gpc3* induces the degradation of extracellular Ihh.

We also used real-time RT–PCR to compare the relative mRNA levels of the two well-characterized Hh targets GLI1 and PTC1 in bones. Fig 3E shows that levels of both Hh targets are significantly higher in *Gpc3*-null embryonic bones. The increase of PTC1 in the mutant bones was confirmed by immunohistochemistry (Fig 3D). The levels of GLI1 protein could not be assessed due to the high background generated by the commercially available antibodies. In addition, we verified that the *Gpc3*-null mice express higher levels of the parathyroid hormone-related protein (PTHrP), a well-characterized target of Ihh in the bone, which is specifically expressed by the perichondrial cells and chondrocytes at the end of the bone (Fig 3D; Kronenberg, 2003). Taken together, these results clearly show that the Hh signalling pathway is hyper-activated in the bone of *Gpc3*-null mice. Consistent with our data, cartilage-restricted Ihh-overexpressing mice show upregulation of PTC expression in the chondrocytes and perichondrium (Long *et al*, 2003), and PTHrP in the periarticular area (Kobashashi *et al*, 2005), with the consequent increase in chondrocyte proliferation (Long *et al*, 2001) and longitudinal growth plate expansion.

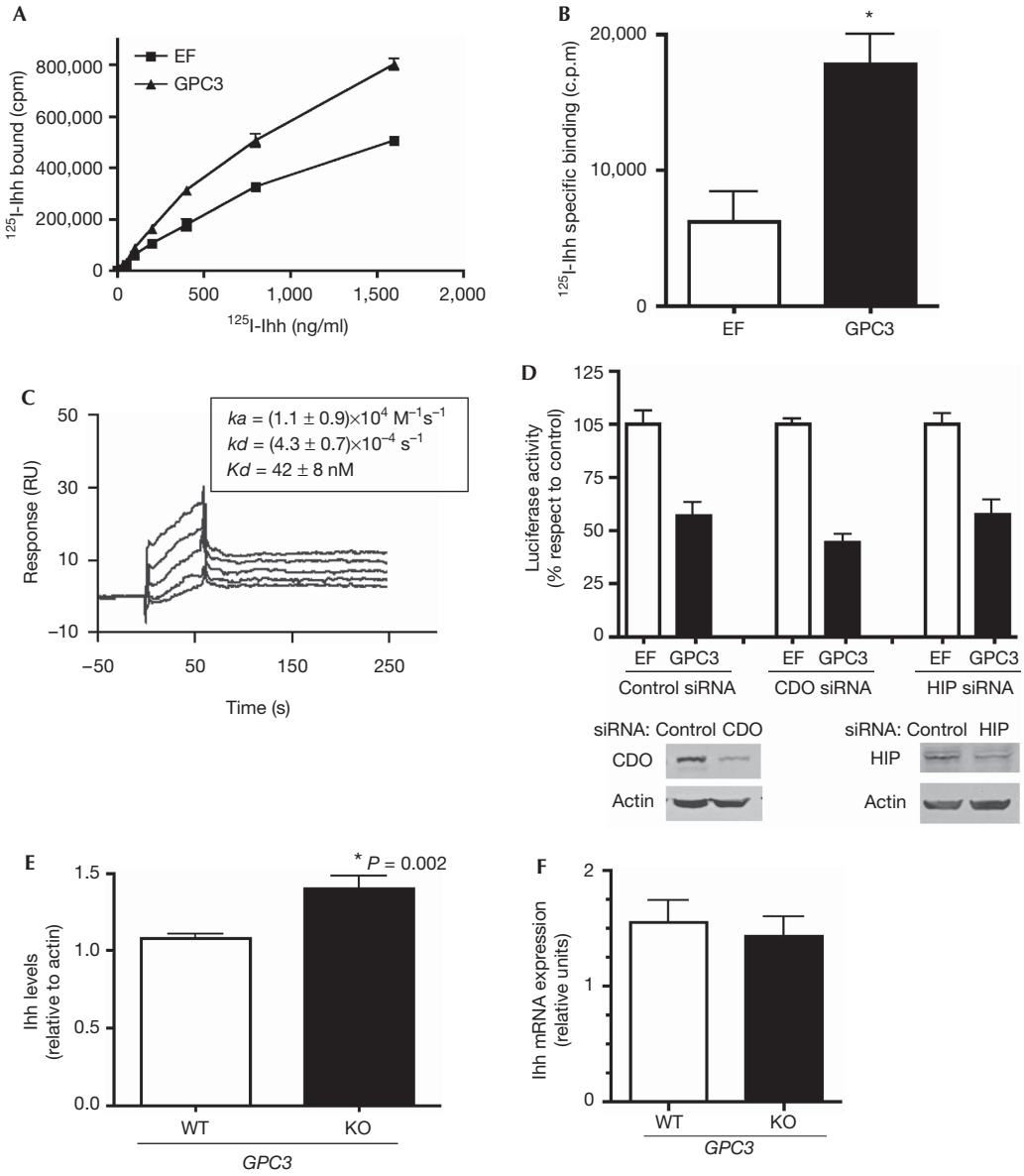

Fig 2 | Characterization and consequences of GPC3–lhh interaction. (**A–C**) Ihh binds to GPC3. (**A**) Binding of ^{125}I-Ihh to human embryonic kidney (HEK)293T cells transfected with GPC3 expressing vector or vector controls (EF). A representative experiment of three is shown: points, average of triplicates; bars, ± s.d. (**B**) The specific binding of ^{125}I-Ihh to HEK293T cells transfected with GPC3 or EF was determined in the presence of 100 × unlabelled Ihh. Bars: average of triplicates + s.d.; asterisk: statistically significant difference. (**C**) SRP analysis of the GPC3–Ihh interaction. GPC3ΔGPI was immobilized in the flow cell into streptavidin-coated SA sensor chips, and various concentrations of Ihh (bottom to top: 15, 30, 60, 120 and 240 nM) were injected on the surface of flow cells. The nonspecific binding was subtracted from the sensogram. Inset: *ka*, *kd* and *Kd* values were determined using a 1:1 Languimuir binding model. Each value is expressed as the mean ± s.e. of five different concentrations. (**D**) GPC3 inhibits Hh signalling independently of CDO and HIP. Top: NIH 3T3 cells were transfected with a GPC3 or EF along with a luciferase reporter vector driven by an Hh responsive promoter (8Xgli) and β-galactosidase. As indicated, siRNA for silencing CDO siRNA, HIP siRNA or non-targeting control siRNA was also transfected. Cells were stimulated for 48 h with Shh- or control-conditioned medium and luciferase and β-galactosidase assays carried out. For each siRNA condition, the fold stimulation induced by Hh in EF-transfected cells was considered to be 100%. Bars represent the luciferase activity as percentage of the control (average + s.d. of triplicates). Bottom: Western blot for CDO and HIP in NIH 3T3 cells treated as indicated, using actin as loading control. (**E,F**) Increased Ihh levels in GPC3-null mice. (**E**) Western blot analysis of Ihh levels in whole-embryo lysates using actin as loading control was carried out. Bands were then scanned and quantified by densitometry. Average density + s.d. of Ihh/actin ratio is shown. In all three independent litters were analysed. (**F**) Relative levels of *Ihh* transcripts determined by real-time PCR using β-actin transcript levels as reference. Two independent litters were analysed. Bars represent mean + s.d. for the indicated genotypes. CDO, CAM-related/downregulated by oncogenes; EF, elongation factor; GPC3, Glypican 3; Hh, hedgehog; HIP, Hedgehog-interacting protein; Ihh, Indian hedgehog; mRNA, messenger RNA; PCR, polymerase chain reaction; RU, relative units; Shh, sonic hedgehog; siRNA, small interference RNA; SRP, small plasmon resonance; WT, wild type.

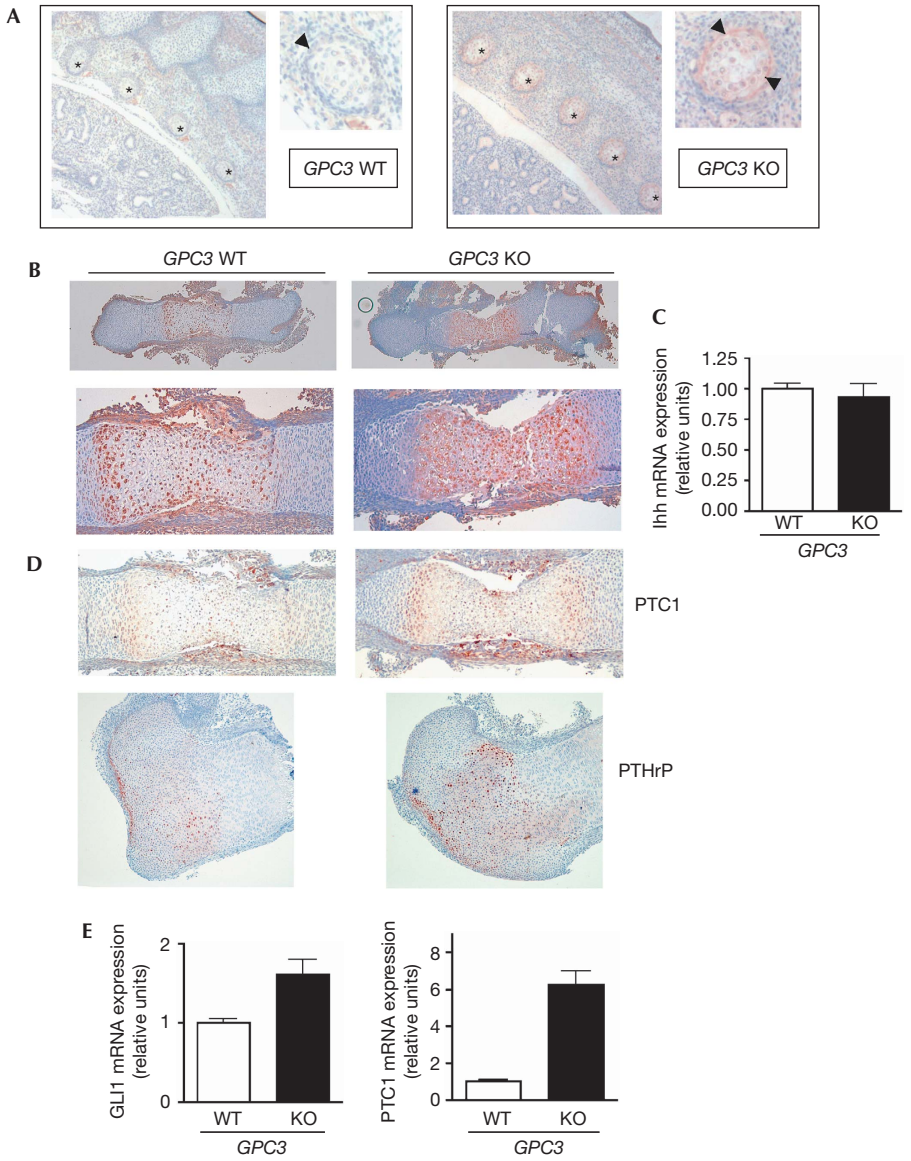

Fig 3 | Increased levels of Indian hedgehog and signalling in the bones of Glypican 3-null mice. Immunohistochemical analysis of Ihh expression in (**A**) embryonic day (E)17.5 embryo sections or (**B**) femur sections dissected from E15 embryos of *Gpc3*-null (GPC3 KO) and normal littermates (GPC3 WT). (**A**) Sagittal sections show staining in the cartilage primordium of ribs (asterisk); a higher magnification to visualize the perichondrium (arrowhead) is shown on the right. (**B**) Whole femur view (magnification: × 25, top) and higher magnification (× 50, bottom) show increased Ihh staining in the GPC3 KO sections. (**C**) Relative femur levels of *Ihh* transcripts determined by real-time RT–PCR using β-actin transcript levels as reference. In all three independent litters with a total of seven wild-type and six GPC3 KO mice were analysed. Bars represent mean + s.d. for the indicated genotypes. (**D**) Immunohistochemical analysis of PTC1 (E15.5) and PTHrP (E17.5) in embryonic femur sections. (**E**) Relative *Gli1* and *Ptc1* transcripts levels determined by real-time RT–PCR. Femurs from four independent litters with a total of 10 wild-type and 8 GPC3 KO mice were analysed. GPC3, Glypican 3; Ihh, Indian hedgehog; KO, knock-out; PTC1, Patched 1; PTHrP, parathyroid hormone-related peptide; RT–PCR, reverse transcriptase polymerase chain reaction; WT, wild type.

Viviano *et al* (2005) previously reported an abnormal persistence of hypertrophic chondrocytes within the diaphysis of GPC3-deficient E16.5 embryonic bones, such that a single continuous hypertrophic zone is seen between the distal and proximal growth plate. Interestingly, we now show that this continuous disorganized proliferating area contains higher levels of Ihh in *Gpc3*-null mice (Fig 3B). Therefore, the accumulation of Ihh as a result of the lack of GPC3 might be the cause of increased cell proliferation and the longer bones observed in the *Gpc3*-null mice (Viviano *et al*, 2005). In this regard, it is important to note that GPC3 is highly expressed in these areas of developing bones (Viviano *et al*, 2005). Taken together, our results indicate that the increased body size of *Gpc3*-null mice is, at least in part, the combined result of higher levels of Ihh, which stimulate bone

growth, and increased levels of Shh, which cause hyperproliferation of other tissues, including the floor plate and the duodenum (Capurro *et al*, 2008); Shh is not expressed in developing bones (supplementary Fig S1 online).

It is interesting to compare our results with those of the paper by Chiao *et al* (2002), who wanted to investigate whether GPC3 regulates body size through the IGF signalling pathway, as it was originally suggested. They followed a similar approach to that used by us to test the involvement of the Hh signalling pathway in the regulation of body size by GPC3: they bred *Gpc3*-null mice with mice deficient in IGF signalling owing to the lack of IGF2, IGFI or IGFI receptor—similar to the *Ihh*-null mice, all these mutants are smaller than normal. In all cases the overgrowth induced by the lack of GPC3 in mice with deficient IGF signalling was similar (as a percentage) to that observed in the single GPC3 mutants, and the authors concluded that GPC3 regulates embryo size independently of the IGF signalling system.

In summary, here we present conclusive genetic evidence that the Hh signalling pathway mediates, at least in part, the regulatory role of GPC3 in the regulation of embryonic growth. In addition, our biochemical and expression studies provide support for a model in which the capacity of GPC3 to inhibit Ihh signalling is based on its ability to bind to Ihh at the cell membrane, and to induce Ihh endocytosis and degradation. We conclude that the overgrowth observed in the SGBS patients is, in part, due to the increased activity of Ihh caused by the lack of functional GPC3.

METHODS

Mouse strains. The *Ihh*$^{+/-}$ mice (129-*Ihh*^{tm1Amc}/J) were purchased from The Jackson Laboratory (Bar Harbor, ME, USA), and the *GPC3*$^{+/-}$ mice have been described previously (Cano-Gauci *et al*, 1999). C57BL/6 wild-type mice were obtained from Charles River Canada Laboratories (St Constant, QC, Canada). All mice were genotyped by PCR.

Breeding of mutants. *Ihh* heterozygous mice were repeatedly mated with wild-type C57BL/6 mice to obtain the *Ihh*$^{-}$ mutation in a high C57BL/6 genetic background (at least 87.5%), in which the *Gpc3* mutant phenotype is more severe (Cano-Gauci *et al*, 1999). Double *Ihh–Gpc3* heterozygous mice were then obtained by mating male *Ihh*$^{+/-}$ with female *GPC3*$^{+/-}$. Finally, double *Ihh/Gpc3* knock-out embryos were generated by crossing female *GPC3*$^{+/-}$; *Ihh*$^{+/-}$ with male *GPC3*$^{+/Y}$; *Ihh*$^{+/-}$. The body weights of E16.5–E18.5 embryos were obtained immediately after dissection. Tail tip samples were then collected and subsequently genotyped by PCR. For each embryo, the relative body weight was normalized by considering the average weight of wild-type embryos in the corresponding litter as 1.

Western blot analysis. E11.5–E13.5 embryos were dissected out of their yolk sacs and genotyped. Embryo extracts were prepared as described previously (Song *et al*, 2005), and the levels of Ihh (C-15, Santa Cruz, Santa Cruz, CA, USA), Shh (H-160, Santa Cruz) and β-actin (AC-40, Sigma, St Louis, MO, USA) were assessed by Western blot. NIH 3T3 cell lysates were prepared with radio immunoprecipitation assay (RIPA) buffer and the levels of CDO (AF2429, R&D, Minneapolis, MN, USA), HIP (R-20, Santa Cruz) and β-actin determined by Western blot.

RNA interference and Gli reporter assay. The Gli reporter assay was carried out in NIH 3T3 cells as described previously (Capurro *et al*, 2008). To silence CDO or HIP, 100 nM of CDO siRNA (sc-60346, Santa Cruz), HIP siRNA (sc-40164, Santa Cruz) or non-targeting control siRNA A (sc-37007, Santa Cruz) was transfected using DharmaFECT-1 transfection reagent (Dharmacon, Chicago, IL, USA). β-Galactosidase activity was used to normalize the transfection efficiencies. For each siRNA condition, results are presented as a percentage of the luciferase activity measured after transfection with vector control (elongation factor (EF)). siRNA-mediated knockdown of CDO and HIP was confirmed in parallel wells by Western blot analysis.

Quantitative real-time RT–PCR. Total RNA was isolated from E13.5 embryos or dissected femurs obtained from E16.5–E18.5 embryos, and cDNA was then generated by reverse transcription using oligo(dT)$_{12-18}$ primers (Invitrogen, Burlington, ON, Canada). Quantification of *Ihh*, *Ptc1* and *Gli1* mRNA expression was carried out with the ABI Prism 7000 Sequence Detection System (Applied Biosystems, Foster City, CA, USA) using QuantiTect™ SYBR® Green (Qiagen, Valencia, CA, USA). Data were normalized against the transcription levels of β-actin. Primers used for Ihh were as follows: Ihh, forward: 5′-CCCCAACTACAATCCCGACATC-3′; and reverse: 5′-CGCCAGCAGTCCATACTTATTTCG-3′. The sequence of primers used for PTC1, Gli1 and β-actin detection was reported previously (Capurro *et al*, 2008).

Immunohistochemical analysis. Paraffin-embedded embryo sections were prepared from *Gpc3*-null embryos and normal littermates following standard procedures. When indicated, the limbs were dissected from the embryos before the preparation of the tissue sections. Ihh expression was assessed by immunostaining the tissue sections with a goat anti-Ihh polyclonal antibody (C-15, Santa Cruz) using the Cell and Tissue Staining kit (Goat kit, R&D). PTC1 and PTHrP immunostaining was carried out with anti-PTC1 (H-267, Santa Cruz) or anti-PTHrP (H-137, Santa Cruz) rabbit polyclonal antibodies and Histostain SP for aminoethylcarbazole (AEC) kit (Zymed Laboratories, South San Francisco, CA, USA). In all, four independent litters were analysed and representative sections are shown.

Ihh iodination and binding assay. Recombinant Ihh (amino terminal peptide C28II, R&D) was iodinated with 1 mCi of Iodine-125 (Perkin-Elmer, Waltham, MA, USA) using Iodo-Gen precoated reaction tubes (Pierce, Rockford, IL, USA). For the binding assay, HEK293T cells were seeded in 48-well plates at a density of 75,000 cells per well, and transfected with GPC3 or control expression vectors using Lipofectamine 2000 (Invitrogen). At 24 h after transfection, cells were washed twice with ice-cold serum-free medium, and binding solution containing different concentrations of ^{125}I-Ihh (range 25–1,600 ng/ml) in ice-cold serum-free medium was added for 3 h at 4 °C. The binding solution was then removed and the cells were gently washed three times, lysed in 0.2 N NaOH for 15 min and the radioactivity in the extracts was counted in a gamma counter. To determine the specific binding, GPC3- or control-transfected cells were incubated with a binding solution containing 50 ng/ml of ^{125}I-Ihh supplemented with a 100 × excess of unlabelled Ihh (5 μg/ml) for 3 h at 4 °C. The cell samples were then processed as described above. The experiments were carried out three times in triplicate.

Surface plasmon resonance analysis. The kinetic constants of the interaction of Ihh with GPC3 were evaluated using a BIAcore 3000 biosensor system (Biacore Life Sciences, Piscataway, NJ, USA). The His-tagged soluble form of GPC3 (GPC3ΔGPI/His) was biotinylated with EZ-link™Sulfo-NHS-LC-biotin (Pierce) and

immobilized (1,000 RU) in flow-cell two on a streptavidin sensorship (Biacore AB). Flow-cell one, without ligand, was used as a correction reference for nonspecific binding. The indicated concentrations of Ihh (R&D) in running buffer (10 mM Hepes pH 7.4, 0.15 M NaCl, 1.8 mM $CaCl_2$, 0.005% (v/v) surfactant P20) were injected over these flow cells at 50 μl/min for 60 s at 25 °C. After a 3-min wash with running buffer, the flow cells were regenerated with 1-min pulses of running buffer containing 1 M NaCl and 10 mM NaOH.

Supplementary information is available at *EMBO reports* online (http://www.emboreports.org).

ACKNOWLEDGEMENTS

This work was funded by the Canadian Institute of Health Research.

CONFLICT OF INTEREST

The authors declare that they have no conflict of interest.

REFERENCES

Cano-Gauci DF *et al* (1999) Glypican-3-deficient mice exhibit the overgrowth and renal abnormalities typical of the Simpson–Golabi–Behmel syndrome. *J Cell Biol* **146:** 255–264

Capurro MI, Xu P, Shi W, Li F, Jia A, Filmus J (2008) Glypican-3 inhibits hedgehog signaling during development by competing with Patched for Hedgehog binding. *Dev Cell* **14:** 700–711

Chiao E, Fisher P, Crisponi L, Deiana M, Dragatsis I, Schlessinger D, Pilia G, Efstratiadis A (2002) Overgrowth of a mouse model of the Simpson–Golabi–Behmel syndrome is independent of IGF signaling. *Dev Biol* **243:** 185–206

Desbordes SC, Sanson B (2003) The glypican Dally-like is required for hedgehog signalling in the embryonic epidermis of *Drosophila*. *Development* **130:** 6245–6255

Ehlen HWA, Buelens LA, Vortkamp A (2006) Hedgehog signaling in skeletal development. *Birth Defects Res* **78:** 267–279

Gorlin RJ (1995) Nevoid basal cell carcinoma syndrome. *Dermatol Clin* **13:** 113–125

Han C, Belenkaya TY, Wang B, Lin X (2004) *Drosophila* glypicans control the cell-to-cell movement of hedgehog by a dynamin-independent process. *Development* **131:** 601–611

Kobashashi T, Soegiarto DW, Yang Y, Lanske B, Schipani E, McMahon AP, Kronenberg HM (2005) Indian Hedgehog stimulates periarticular chondrocyte differentiation to regulate growth plate length independently of PTHrP. *J Clin Invest* **115:** 1734–1742

Kronenberg HM (2003) Developmental regulation of the growth plate. *Nature* **423:** 332–336

Long F, Chung U, Ohba S, McMahon J, Kronenberg HM, McMahon AP (2003) Ihh signaling is directly required for the osteoclast lineage in the endochondral skeleton. *Development* **131:** 1309–1318

Long F, Zhang XM, Karp S, Yang Y, McMahon AP (2001) Genetic manipulation of hedgehog signaling in the endochondral skeleton reveals a direct role in the regulation of chondrocyte proliferation. *Development* **128:** 5099–5108

Lum L, Yao S, Mozer B, Rovescalli A, Von Kessler D, Nirenberg M, Beachy PA (2003) Identification of hedgehog pathway components by RNAi in *Drosophila* cultured cells. *Science* **299:** 2039–2045

Milenkovic L, Goodrich LV, Higgins KM, Scott MP (1999) Mouse patched controls body size determination and limb patterning. *Development* **126:** 4431–4440

Nieuwenhuis E, Hui CC (2005) Hedgehog signaling and congenital malformations. *Clin Genet* **67:** 193–208

Oliver F, Christianis JK, Liu X, Rhind S, Verma V, Davison C, Brown SDM, Denny P, Keightley PD (2005) Regulatory variation at glypican-3 underlies a major growth QLT in mice. *Plos Biol* **3:** e135

Paine-Saunders S, Viviano BL, Zupicich J, Skarnes WC, Saunders S (2000) Glypican-3 controls cellular responses to Bmp4 in limb patterning and skeletal development. *Dev Biol* **225:** 179–187

Pilia G, Hughes-Benzie RM, MacKenzie A, Baybayan P, Chen EY, Huber R, Neri G, Cao A, Forabosco A, Schlessinger D (1996) Mutations in GPC3, a glypican gene, cause the Simpson–Golabi–Behmel overgrowth syndrome. *Nat Genet* **12:** 241–247

Song HH, Shi W, Xiang Y, Filmus J (2005) The loss of Glypican-3 induces alterations in Wnt signaling. *J Biol Chem* **280:** 2116–2125

St-Jacques B, Hammerschmidt M, McMahon AP (1999) Indian hedgehog signaling regulates proliferation and differentiation of chondrocytes and is essential for bone formation. *Genes Dev* **13:** 2072–2086

Viviano BL, Silverstein L, Pflederer C, Paine-Saunders S, Mills K, Saunders S (2005) Altered hematopoiesis in glypican-3-deficient mice results in decreased osteoclast differentiation and a delay in endochondral ossification. *Dev Biol* **282:** 152–162

Zhang XM, Ramalho-Santos M, McMahon AP (2001) Smoothened mutants reveal redundant roles for Shh and Ihh signaling including regulation of L/R asymmetry by the mouse node. *Cell* **105:** 781–792